Characterizing tropospheric O_3 and CO around Frankfurt over the 1994-2012 period based on MOZAIC-IAGOS aircraft measurements

H. Petetin[1], V. Thouret[1], A. Fontaine[1], B. Sauvage[1], G. Athier[1], R. Blot[1], D. Boulanger[1], J.-M. Cousin[1], P. Nedelec[1]

(1) {Laboratoire d'Aérologie, Université de Toulouse, CNRS, UPS, France}

Correspondence to: H. Petetin (herve.petetin@aero.obs-mip.fr)

Abstract

In the framework of the MOZAIC-IAGOS program, ozone and carbon monoxide vertical profiles are available since 1994 and 2002, respectively. This study investigates the variability and trends of both species at several tropospheric layers above the Frankfurt and Munich airports. About 21,300 flights have been performed over the 1994-2012 period, which represents the densest dataset in the world (about 96 flights per month on average). The mean ozone vertical profile shows a strong vertical gradient in the first kilometre (deposition, titration by NO) during the whole year and close to the tropopause (stratosphere-troposphere exchanges) in spring and summer. The mean CO vertical profile is characterized by a strong decrease of the concentrations in the first kilometre, in particular in winter and autumn, and a moderate one higher in the troposphere. In terms of seasonal variations, the mean O_3 has a minimum in November-December in the whole troposphere, a broad spring/summer maximum in the lower and mid-troposphere and a sharp maximum in summer in the upper troposphere. The mean CO seasonal profile shows a broad minimum in July-October close to the surface, refined to September-October higher in the troposphere, while maximum concentrations occur in February-April in the whole troposphere. Over the 1994-2012 period, the mean O_3 trends are mostly insignificant at a 95% confidence level, except in winter where a slightly significant increase (from +0.83[+0.13;+1.67]% yr^{-1} in the LT to +0.62[+0.02;+1.22]% yr^{-1} in the UT, relatively to the reference year 2000) is found. The O_3 5th percentile shows similar upward trends at the annual scale in all tropospheric layers. All trends remain insignificant for the O_3 95th percentile. Conversely, the mean CO as well as its 5th and 95th percentiles are decreasing both at the annual scale and at the seasonal scale in winter, spring and summer (although not always in all tropospheric layers) with trends ranging between -1.22[-2.27;-0.47] and -2.63[-4.54;-1.42]% yr^{-1}, relatively to the reference year 2004). However, all CO trends remain insignificant in autumn.

The changes in the O_3 seasonal cycle are also investigated, with a focus on the phase. Ozone maxima occur earlier and earlier with a shift around -12.1±4.1 days $decade^{-1}$ in the lower

troposphere, in general agreement with previous studies. The analysis of other ozone datasets in Europe (including surface stations and ozone soundings) confirms this trend, but highlights strong heterogeneities in the changes of phase from one site to the other. Interestingly, this seasonal shift is shown to decrease with the altitude, with values of -5.2±2.3 and -2.3±2.1 days decade^{-1} in the mid- and upper troposphere, respectively.

1 Introduction

As one of the major sources of hydroxyl radicals (OH) that directly control the atmospheric lifetime of a large number of compounds, ozone (O_3) plays a unique role in the oxidative capacity of the atmosphere. In the troposphere, it acts as a powerful greenhouse gas with a positive radiative forcing (RF) of 0.40±0.20 W m^{-2} that is not compensated by the RF of stratospheric ozone estimated at -0.05±0.10 W m^{-2} (IPCC, 2013). It also has well-known adverse impacts on human health (Jerrett et al., 2009), vegetation (Ashmore, 2005; Paoletti, 2006) and agricultural crop yields (Van Dingenen et al., 2009). In the troposphere, O_3 is formed by photochemical reactions implying various compounds including volatile organic compounds (VOC), carbon monoxide (CO) and nitrogen oxides (NO_x), and it can be removed by photolysis, dry deposition and uptake on aerosols (Moise and Rudich, 2000, 2002). Despite the considerable scientific achievements made during the last decades, the O_3 budget remains difficult to quantify precisely (Wu et al., 2007). Major uncertainties are related to lightning NO_x production, isoprene biogenic emissions and degradation chemistry, biomass burning emissions, water vapour concentrations and stratosphere-troposphere exchanges (Stevenson et al., 2006). This leads to a large heterogeneity of the O_3 abundance and variability in the troposphere, making it difficult to draw a simple and global picture of the O_3 present-day concentrations and trends.

During the last decades, ozone trends in the free troposphere have been intensively investigated, notably based on ozonesonde long-term observations. Specifically in Europe where such measurements are available over a few decades at several sites (e.g., Hohenpeissenberg, Payerne, Uccle, De Bilt, Legionowo, Lindenberg), most results indicate an increase of ozone levels from the 1960s until the mid-1980s (Logan et al., 1999; Oltmans et al., 1998; Tiao et al., 1986), the only site with no significant trend being Lindenberg, Germany, for the 1975-1983 period (Tiao et al., 1986). Such positive trends were found all along the year without any significant seasonal influence (Logan et al., 1999) and through the entire tropospheric column (Logan et al., 1999; Oltmans et al., 1998). By the mid-1980s until 2000s, most ozonesonde observations in Europe indicate a progressive levelling-off of ozone concentrations in the free troposphere (Logan et al., 1999; Oltmans et al., 1998, 2006; Gaudel et al., 2015). For instance, the significant positive trends obtained at Hohenpeissenberg in the entire tropospheric column for 1971-2010 vanish in most

tropospheric layers considering the 1981-2010 period (Oltmans et al., 2013). Ozone observations at Jungfraujoch, Switzerland (3850 m), an elevated alpine site supposed to be representative of the free troposphere, indeed reveal that concentrations have continued to increase in the 1990s, in particular during winter, the levelling-off occurring only in the 2000s (Cui et al., 2011). A similar evolution is reported by Cooper et al. (2014) at other mountain or remote sites in Europe, and by Logan et al. (2012) on the observations by the MOZAIC (Measurements of OZone and water vapour by Airbus In-service airCraft) aircraft above some European airports.

A full understanding of the ozone variability would ideally require to discriminate and quantify all the terms of the ozone budget. This can be easily achieved with determinist numerical models, but the confidence in the results remains limited by the high uncertainties at stake in both models and input data. An alternative but more qualitative approach consists in taking benefit from the different seasonal patterns of the various ozone budget terms (e.g., precursors emissions, photochemical production, stratospheric intrusions, transport regimes) and aims at linking the evolution of the ozone seasonality to changes in the contribution of its various sources and sinks. At the Mace Head coastal site during the 1987-2003 period, Simmonds et al. (2004) found the highest ozone increase in both polluted continental (originating from Europe) and baseline (originating from the Northern Hemispheric marine boundary layer) air masses during the winter while baseline ozone levels increased noticeably less during the summer, and do not show any significant trend in polluted air masses. Extending the analysis to the 1988-2012 period, Derwent et al. (2013) noticed that the still increasing baseline ozone levels do not extend to the European ozone load that levelled-off during the 2000s. These results thus suggest a possible compensation between a decrease of ozone local formation in Europe and an increase of ozone imports. At several remote or alpine sites in northern mid-latitudes, Parrish et al. (2013) recently highlighted a noticeable shift in the ozone cycle at ground, the maximum daily ozone occurring between 3 and 6 days earlier each decade since the 1970s. Such a shift may reflect some changes in the contributions of the various ozone sources and sinks, e.g., transport pathways, precursors emissions, photochemistry or climate change impacts (Parrish et al., 2013). The present study aims at characterizing the vertical distribution, the temporal variability, the seasonality and the trends of tropospheric ozone in Central/Western Europe. Based on vertical profiles measured by commercial aircraft involved in the MOZAIC-IAGOS (In-service Aircraft for a Global Observing System) program, it will focus on the free and upper troposphere in order to go beyond the more limited representativeness of measurements in the boundary layer measurements (close to precursors emissions and/or deposition sink) at the regional scale. However, results in the boundary layer will be also presented to give a full picture of the troposphere. This study will also investigate the variability and trends of carbon monoxide, one of the main O_3 precursors measured in the framework of the MOZAIC-IAGOS program. As a long lifetime (several weeks to several months) compound emitted by incomplete combustion processes, carbon

monoxide represents an interesting pollution tracer able to provide useful information on long-range transport at the hemispheric scale. Characterizing carbon monoxide in troposphere may thus help investigating the variability and trends affecting ozone.

Section 2 presents the MOZAIC-IAGOS dataset used in this paper and describes the treatment applied on vertical profile data. The vertical distribution, the seasonal variations, the trends of O_3 and CO and the changes affecting the O_3 seasonal cycle are analysed in Sect. 3. Main results and conclusions are summarized in Sect. 4.

2 Data and methodology

2.1 MOZAIC-IAGOS dataset

In the framework of the MOZAIC-IAGOS program (www.iagos.fr), ozone and carbon monoxide measurements (among other parameters) are performed by commercial aircraft along various flight routes in the world (most of them from or to European airports) since 1994 and 2002, respectively. Until October 2014 (date of the last MOZAIC aircraft flight), both ozone and carbon monoxide have been measured using the same instruments in all aircraft, thus ensuring the dataset consistency during most of the period. Ozone measurements were performed using a dual-beam UV-absorption monitor (time resolution of 4 seconds) with an accuracy estimated at about ±2 ppbv / ±2% (Thouret et al., 1998). Carbon monoxide was measured by an improved infrared filter correlation instrument (time resolution of 30 seconds) with a precision estimated at ±5 ppbv / ±5% (Nedelec et al., 2003). Note also that comparisons between the MOZAIC ozone dataset and other types of data (e.g., mountain surface stations, ozonesonde) have been performed in Europe, showing a good consistency (Logan et al., 2012; Staufer et al., 2013, 2014).

As MOZAIC aircraft have been retired from service, the European partners involved prepared since years the technical successor in the framework of the European Commission (EC) funded IAGOS program (Petzold et al., 2015). A new concept of aircraft system and instruments has been developed and installed on Airbus long-range aircraft (A340 or A330), starting from July 2011. Six aircraft are actually in operation with IAGOS systems. The new IAGOS instrumentation for O_3 and CO is extensively described in Nédélec et al. (2015). Briefly, the O_3 and CO measurements are based on the same technology used for MOZAIC, with the same estimated accuracy and the same data quality control. The nearly 4 years overlap of “old” MOZAIC and “new” IAGOS systems operations allowed to prove that the new IAGOS systems provide the same data quality, which is especially important for trends analysis.

The present study will focus on the Frankfurt airport where the longest (from 1994 to 2012) and densest (18,598 flights) record is available. In order to fill a large data gap in 2005, this dataset is combined to the data from the Munich airport (2,734 flights, mostly between 2002 and 2005),

approximately 300 km South-East from Frankfurt, as done in several previous studies (Logan et al., 2012; Zbinden et al., 2006, 2013). Note also that no measurements are available during a part of 2010 due to instrumental problems. An illustration of the dataset density by month and year is shown in Fig. S1 and S2 in the Supplement.

2.2 Tropopause altitude and tropospheric layers

This paper focuses on the analysis of tropospheric vertical profiles obtained over Europe (Germany) during both ascent and descent. As tropospheric air masses are subject to very different constraints depending on their altitude (e.g., distance from surface emissions or stratosphere), the troposphere is divided here in three layers: the lower troposphere (LT), the mid-troposphere (MT) and the upper troposphere (UT). The UT is defined here as the 60 hPa-width layer below tropopause plus 15 hPa, as in Thouret et al. (2006). The MT is delimited by the UT lower boundary and an arbitrarily fixed altitude of 2 km. Data collected in the 1-2 km layer are finally assigned to the LT, the first kilometre above surface being ignored to limit the representativeness degradation induced by emissions over the airport area (confirmed by large enhancements of CO concentrations near the ground in most vertical profiles).

The tropopause altitude can be estimated by several approaches, e.g., thermal, dynamic, chemical criteria (Thouret et al., 2006) or a combination of them (Stohl et al., 2003b). In this paper, we consider the dynamical tropopause, delimited by a potential vorticity (PV) of 2 pvu (1 pvu = 10^{-6} K m^2 kg^{-1} s^{-1}) (see the tropopause height over the 1994-2012 period in Fig. S3 in the Supplement). Two parameters, the PV and the pressure at which PV reaches 2 pvu (so-called $p_{PV=2}$), are derived along all MOZAIC flight routes based on the European Centre for Medium-Range Weather Forecasts (ECMWF) operational analysis (00:00, 06:00, 12:00, 18:00 UTC) and forecasts (03:00, 09:00, 15:00, 21:00 UTC). The $p_{PV=2}$ parameter is used to determine the DT pressure at the top of the selected tropospheric vertical profile.

Tropospheric vertical profiles are selected according to several criteria:

(i) Distance from the airport: Take-offs and landings do not correspond sensu stricto to vertical profiles as aircraft travel some distance before reaching their cruise altitude. In order to limit the uncertainties induced by a potential horizontal heterogeneity, a maximum distance of 400 km from the airport is fixed for the vertical profile data selection. In practice, such a distance is sufficient for sampling the entire vertical profile in most flights, and remains reasonable considering the fact that the ozone vertical variability is expected to be higher than the horizontal one. A sensitivity test with a distance threshold of 800 km leads to differences of mean O_3 concentration in the UT below 3% at the seasonal and annual scale.

(ii) Potential vorticity: Based on PV vertical profiles, the 2 pvu value is used to locate the top of the tropospheric vertical profiles. This is illustrated in Fig. 1 with the flight from Frankfurt to Boston on the 19 March 2002 during which the DT altitude is estimated at 8.8 km. If the distance criterion is fulfilled before reaching DT, the $p_{PV=2}$ parameter is used to estimate the DT pressure (and thus to determine to which tropospheric layer points belong). However, PV values above 2 pvu may sometimes be encountered in the lower troposphere — due to recent deep stratospheric intrusions or convective processes — before decreasing again below the 2 pvu threshold until the tropopause. To avoid a misevaluation of the DT altitudes in such cases, PV values are not considered point by point but over a window of several points — in our case, 60 points, which approximately corresponds to 1800 m on the vertical — and the tropopause is considered to be reached only when the minimum PV over that window exceeds 2 pvu (this value of 60 being empirically chosen to handle most of these situations) (or when the previous criteria is fulfilled) and is set to the bottom of that window. In this study, we are thus considering the real and not purely tropospheric layer, i.e., recent stratospheric intrusions are not filtered in our methodology.

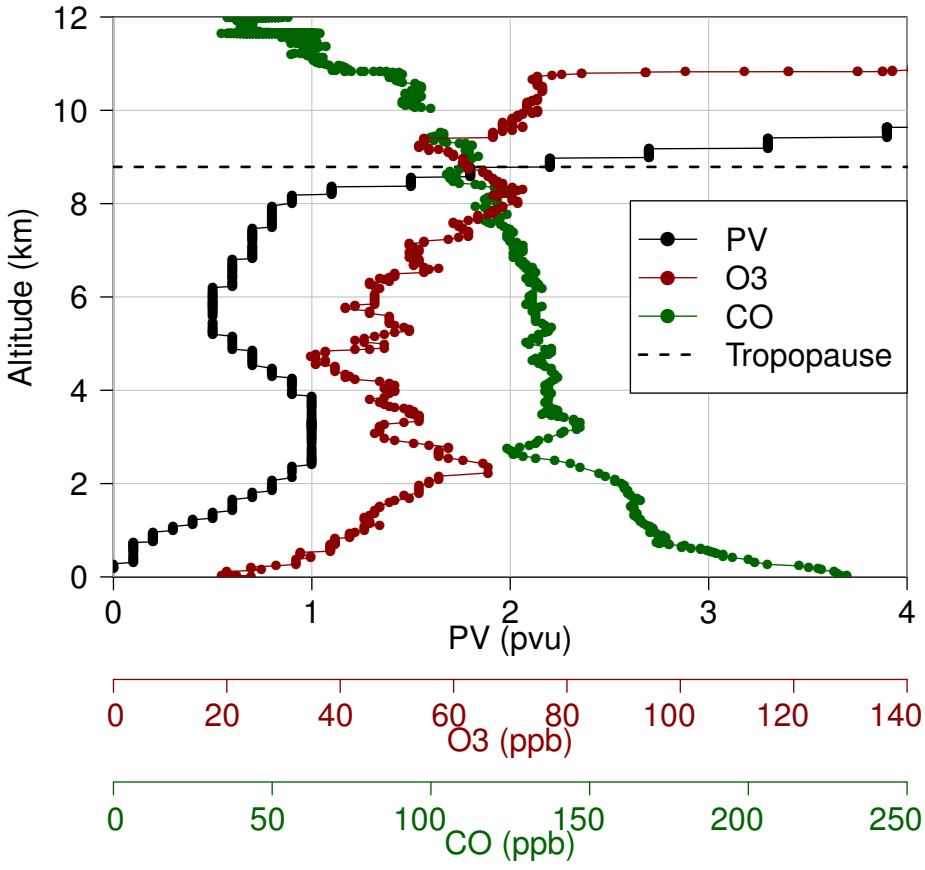

Figure 1: Vertical profile of the potential vorticity (PV), O_3 and CO concentrations during the flight from Frankfurt to Boston on the 19 March 2002 (take-off). The tropopause altitude (dotted black line) is estimated based on PV (see text for the methodology).

It is worth noting that the determination of the tropopause altitude is associated to several uncertainties. Some uncertainties arise from the choice of the method used to locate the tropopause. For instance, the ozone criteria may give a lower dynamical tropopause (DT) compared to the thermal method (Bethan et al., 1996). In the determination of the DT altitude, other uncertainties can arise from the choice of a constant PV to locate the DT. Indeed, Kunz et al. (2011) showed that the PV values at the DT can vary between 1.5 and 5, with higher PV values in summer than in winter. In our case, there are also uncertainties related to the fact that the PV is here a modelled variable. In addition, it is linearly interpolated between PV fields 6-hours apart, which does not allow to entirely catch the variability of the DT. A good example is given in Fig. 1 where the abrupt O_3 increase (corresponding to the tropopause) occurs 2 km above the DT derived from PV values. However, our approach allows to assess in which layer (MT or UT) observations belong even when the tropopause is not reached by the aircraft (within the 400 km around the airport). It is beyond the scope of this study to investigate in more details the influence of the method used to locate the tropopause. Above the Frankfurt airport, a majority of vertical profiles (63%) reach the tropopause while most of the remaining profiles (36%) are selected according to the distance criteria. A similar proportion is found at Munich (63 and 35%, respectively).

2.3 FLEXPART simulations

The FLEXPART Lagrangian particle dispersion model (Stohl et al., 2005) is used to investigate the origin of air masses sampled by the aircraft in the different tropospheric layers above Frankfurt/Munich. Input meteorological data are taken from the ECMWF operational analysis (00:00, 06:00, 12:00, 18:00 UTC) and forecasts (03:00, 09:00, 15:00, 21:00 UTC) and interpolated on a 1°x1° global longitude-latitude grid. The methodology used here basically consists in releasing along each vertical profile 1000 particles every 10 hPa and following them backward in time during 20 days. This duration corresponds approximately to the time during which a pollution plume is expected to remain significantly higher than the tropospheric background (Stohl et al., 2003a). The FLEXPART model computes the particles' residence time, sometimes referred as the potential emissions sensitivity (PES). Output are given on a 1°x1° global longitude-latitude grid, over 1-km width vertical layers up to 11 km plus a remaining layer ranging from 11 to 50 km (i.e., 12 vertical layers). The footprint PES between 0-1 km is presented in Fig. 2 for each tropospheric layer, averaged over the 1994-2012 period. As expected, air masses sampled in the LT spend most of their time in the European boundary layer (mostly in France, Germany, Benelux, England). In the MT, the influence of Europe persists but the influence of North America is greatly enhanced. In the UT, the PES is the highest over North America but stronger winds at these altitudes (e.g. jet streams) also allow a fast transport of air masses from Asia.

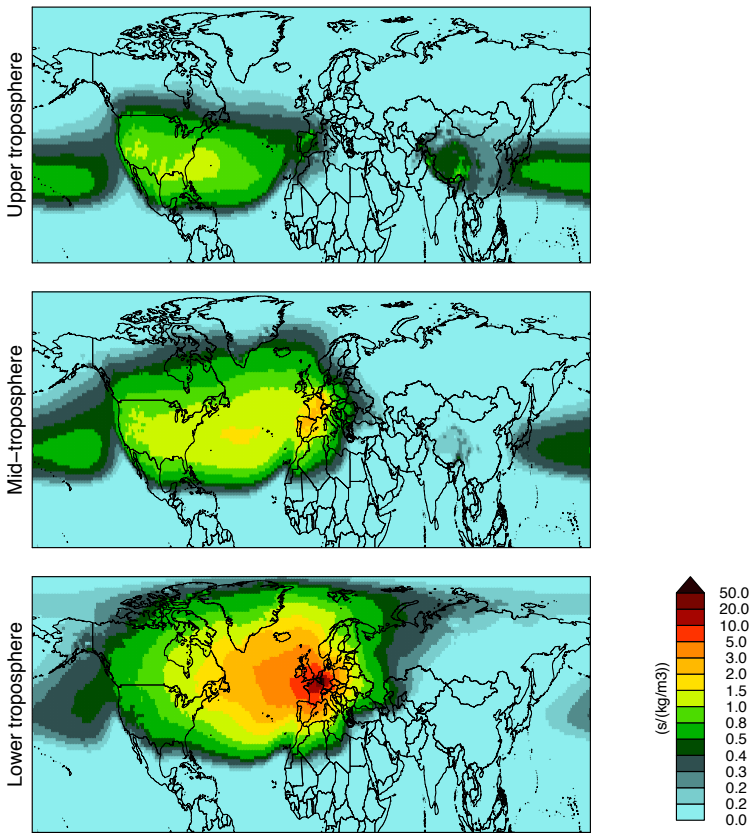

Figure 2: Average residence time (in the first kilometre) of air masses sampled in the three tropospheric layers around Frankfurt between 1994 and 2012. Note the irregular scale.

3 Results

The climatological vertical profiles of O_3 and CO around Frankfurt/Munich are described in Sect. 3.1. The annual and monthly variations of both compounds are analysed in Sect. 3.2. The annual and seasonal trends are investigated in Sect. 3.3. The changes of the O_3 seasonal cycle are explored in Sect. 3.4.

3.1 Climatological vertical profiles

3.1.1 Ozone

Annual and seasonal O_3 and CO climatological vertical profiles are calculated over the whole period (1994-2012 for O_3, 2002-2012 for CO) and shown in Fig. 3. Between the surface (2 km) and the tropopause, the annually-averaged O_3 mixing ratios range between 21-81 (47-81) ppb. Averaged over the entire tropospheric column, the annually-averaged O_3 mixing ratio is 56 ppb. The seasonal variability is strong, with minimum annually-averaged O_3 (over the tropospheric column) in winter (44 ppb) and autumn (48 ppb), and maximum ones in summer (67 ppb) and spring (61 ppb).

The O_3 abundance clearly increases with altitude. The highest vertical gradients are found close to the surface all along the year (dry deposition and titration by NO) and at the vicinity of the

tropopause during spring and summer (exchanges with the stratospheric reservoir). The inflexion of vertical gradients at about 1 km a.g.l. has already been mentioned in Chevalier et al. (2007). In the free troposphere, the vertical gradients are very low in winter and to a lesser extent in autumn, but substantially enhanced during spring and summer where concentrations quickly increase with altitude.

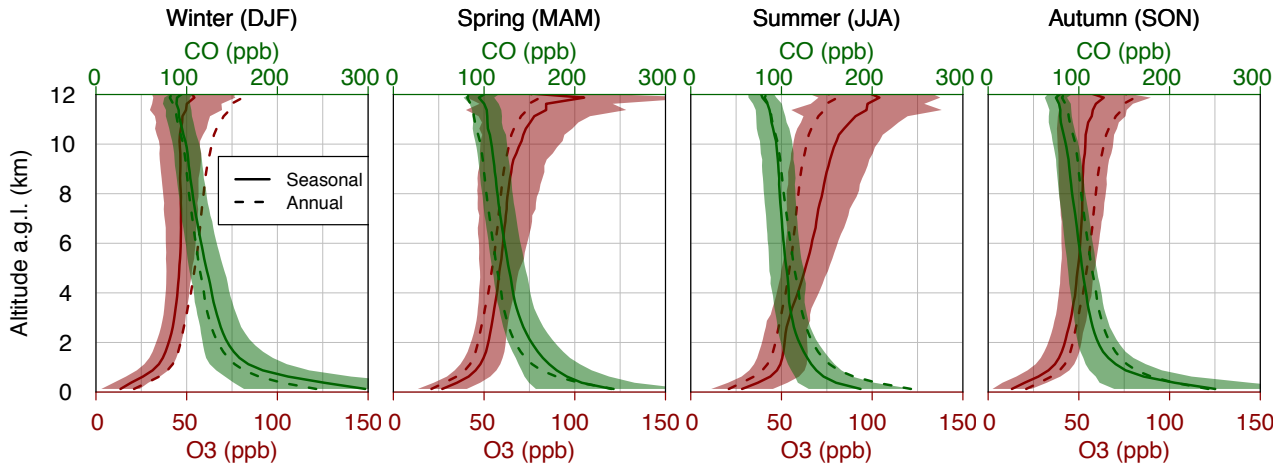

Figure 3: Climatological vertical profiles of O_3 and CO mixing ratios above Frankfurt/Munich per season (continuous lines). Standard deviation is also indicated (filled contour), as well as the overall climatological profile considering all seasons (dotted line, the same for all panels).

At both the annual and seasonal scales, we define the coefficient of variation (CV) as the standard deviation of the daily-averaged concentrations normalized by the corresponding (i.e. annual or seasonal) climatological concentration. Vertical profiles of CV are shown in Fig. 4. The annual CV ranges between 20 and 73% depending on the altitude, with a mean value of 32%. The maximum CVs are found in the first kilometre (73%) and close to the tropopause (53%) where it is likely driven by intense shallow and transient exchanges between the stratosphere and the troposphere (Stohl et al., 2003b). Conversely, the minimum CV is found at about 3.4 km. Rather similar CV vertical profiles are found at the seasonal scale, although with lower values at most altitudes and during most seasons. The minimum seasonal CV is still found at 4.4 km in autumn and between 3.1-3.4 km during the other seasons, thus close to the minimum annual CV. Similarly, the maximum seasonal CVs are found at the surface and close to the tropopause. Interestingly, close to the tropopause, the CV is noticeably higher in spring than during the other seasons, which again, may be due to the day-to-day variability of stratosphere-to-troposphere exchanges that peak during that season.

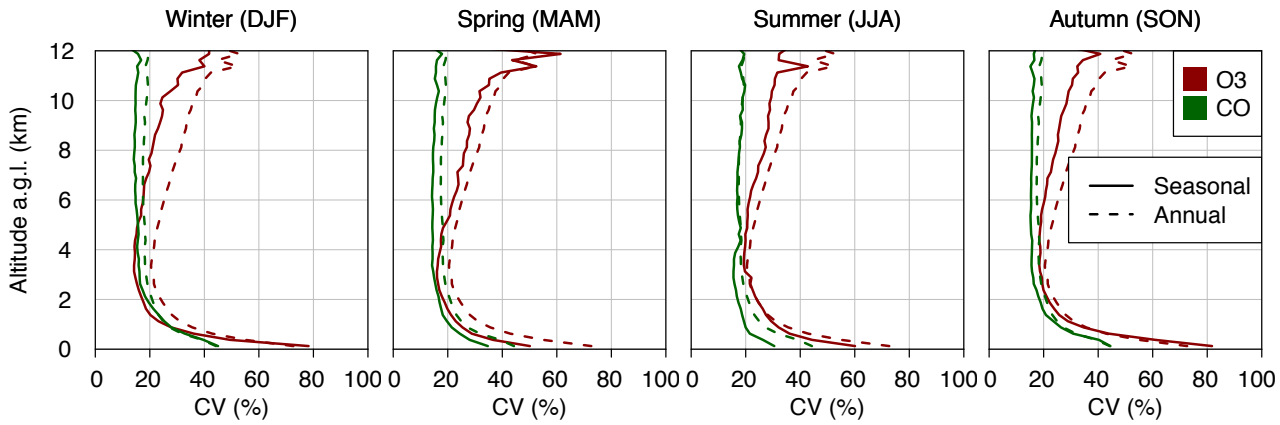

Figure 4: Annual (dotted lines, the same for all panels) and seasonal (continuous lines) coefficient of variation (CV) of daily O_3 and CO mixing ratios above Frankfurt/Munich (see the text for details on the calculation of CVs).

3.1.2 Carbon monoxide

The CO climatological vertical profiles show mixing ratios around 150 ppb at about 1 km and 80 ppb high in altitude. Over the entire tropospheric column, the mean CO mixing ratio reaches 117 ppb. As previously mentioned, the CO mixing ratios in the first kilometre strongly increase as one moves closer to surface emissions (up to 243 ppb at the surface). This concerns first and foremost emissions from the airport area (including aircraft emissions on runways) and potentially emissions from the neighbouring agglomeration. High seasonal variations are observed close to the surface, with concentrations in the first kilometre ranging from 156 ppb in summer to 233 ppb in winter on average. The increase during winter is likely due to a lower vertical mixing and higher emissions. Contrary to O_3, CO does not change significantly from one season to the other in the free troposphere. The seasonal climatological profiles always remain at less than one sigma from the annual climatology (contrary to wintertime O_3 above 4 km). Such moderate seasonal variations in altitude may be due to a higher contribution of secondary sources (biogenic hydrocarbon and methane oxidation) during summer that compensate the decrease of anthropogenic emissions (Holloway et al., 2000).

Concerning the CV (Fig. 4), one can see that CO is less variable than O_3, in particular at the surface and close to the tropopause. The annual CV of CO shows values ranging from 44% close to the surface to 17% in the free troposphere. Interestingly, CV values through the whole free troposphere remain almost constant with altitude. Over the entire tropospheric column, the mean annual CV is 20%. A very similar picture is drawn for the different seasons. The highest values at the surface (in the second half of the troposphere) are encountered in winter/autumn (summer).

3.2 Annual and monthly variations

The average seasonal variations of O_3 and CO in the three tropospheric layers around Frankfurt/Munich are given in Fig. 5, and their annual and monthly time series are shown in Fig. 6.

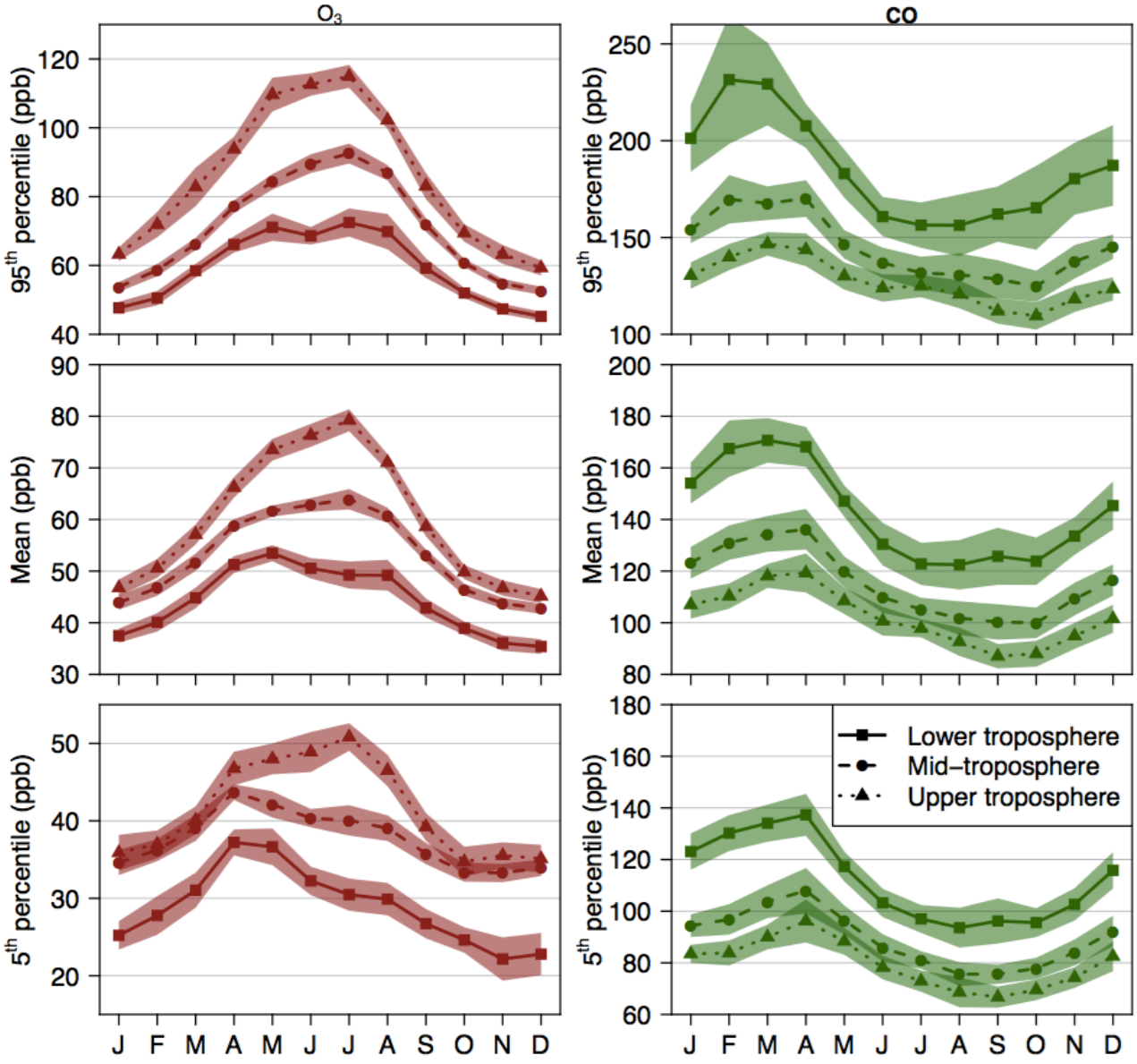

Figure 5: Averaged O_3 (left panels) and CO (right panels) seasonal variations above Frankfurt/Munich in the three tropospheric layers, for the 95th percentile (top panels), the mean (middle panels) and the 5th percentile (bottom panels).

3.2.1 Ozone

As previously noted, the mean tropospheric O_3 increases with altitude, with average mixing ratios (over the whole period) of 44, 53 and 63 ppb in the LT, MT and UT, respectively. A clear seasonal pattern is emphasized in the LT, with a broad spring/summer maximum and a minimum in winter. This is in good accordance with the seasonal variations observed at surface in Europe (Wilson et al., 2012). In the MT and UT, maximum concentrations occur in May and August (highest concentrations in July). Concerning the O_3 5th percentile, different seasonal variations are observed

in the LT and MT where maximum concentrations are encountered in April-May, while the profile in the UT remains quite similar except that concentrations in April are closer to the (maximum) concentrations found in May-July. The 95th percentile shows a maximum in spring/summer in all tropospheric layers (although the profile is sharper in the UT). On average, the monthly mean of the daily O_3 variability (represented by monthly standard deviations in Fig. 6) represents about 20% of the mean in the LT and MT, and 25% in the UT. The highest monthly mean mixing ratios in the LT (above 60 ppb, the 99th percentile) are observed in August 1995, May 1998, August 2003, July 2006 (Fig. 6). The spring 1998 anomaly has been discussed by Koumoutsaris et al. (2008) and is related to the 1997 El Niño that have enhanced stratospheric-tropospheric exchanges (Ordóñez et al., 2007) and pollution export from Asia (higher convective activity and strengthening of the subtropical jet stream) and North America. Anomalies in August 2003 and July 2006 are related to the severe heat waves that struck a large part of Europe (Ordóñez et al., 2005; Solberg et al., 2008; Struzewska and Kaminski, 2008; see also Tressol et al. (2008) for a detailed analysis of the 2003 heat wave with the MOZAIC measurements). Most of these O_3 anomalies in the LT are not always distinguishable in the MT, where the highest concentrations (above 68 ppb, the 99th percentile) are encountered in August 2004 and July 2002, 2006 and 2008. Similarly, the highest monthly concentrations do not always coincide between the MT and UT (see for instance the high O_3 mixing ratio observed in the UT during 2011 and 2012 summers). Nevertheless, on a yearly average, a very similar interannual variability is found between the three tropospheric layers as illustrated by high correlations (R=0.87, 0.75 and 0.94 between the LT/MT, LT/UT and MT/UT, respectively).

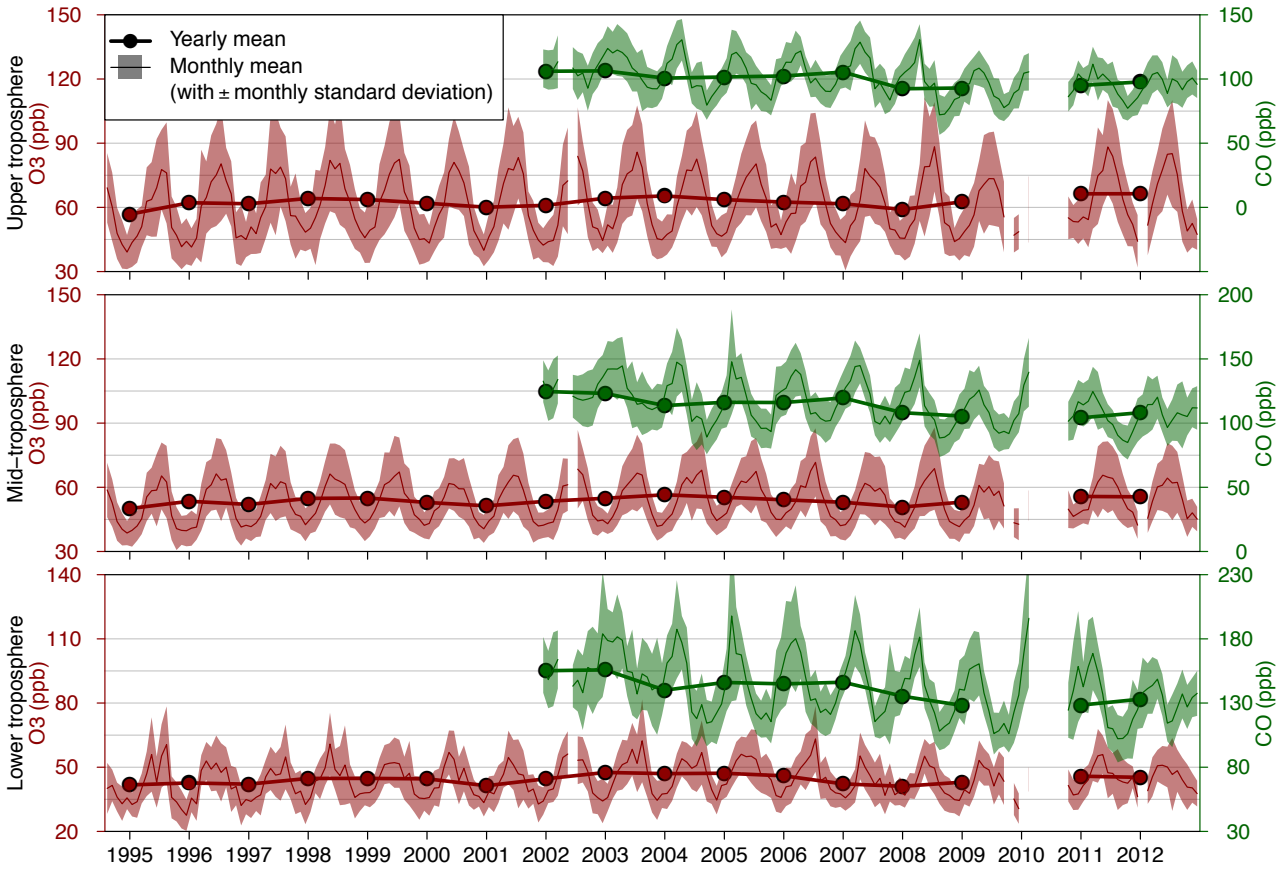

Figure 6: Monthly and yearly mean O_3 and CO concentrations of combined Frankfurt and Munich vertical profiles, in the lower (bottom panel), mid- (middle panel) and upper troposphere (top panel) between 1994 and 2012.

3.2.2 Carbon monoxide

On average, CO mixing ratios of 143, 115 and 101 ppb are found in the LT, MT and UT, respectively. Concentrations in the UT are thus only 29% lower than in the LT (i.e. close to local emissions), which illustrates the high contribution of the CO background at the hemispheric scale. In comparison with O_3, the monthly mean of the daily CO variability is lower and similar in the three tropospheric layers (around 14-16%). Such a result is expected due to the longer lifetime of CO in comparison with O_3, which leads to a higher regional and hemispheric background (Junge, 1974). As shown in Fig. 5, the seasonal cycle of CO is characterized by maximum mixing ratios in late winter/early spring in the whole troposphere. Minimum mixing ratios are encountered in summer/early autumn in the LT and are slightly shifted to late summer/early autumn higher in altitude. Such a seasonal pattern is rather consistent with satellite observations (Worden et al., 2013). It results from a maximum of primary CO emissions in winter (at northern mid-latitudes) associated to a limited photolysis which increases the CO lifetime and allows its accumulation in the atmosphere. This delays the maximum of CO concentrations to late winter/early spring, after which concentrations start to decrease due to a more effective photolytic destruction in summer, despite an enhanced secondary formation from biogenic compounds. A rather similar seasonal pattern is observed with the CO 5^{th} and 95^{th} percentiles except that the peak is sharper (February-March) in the LT for the 95^{th} percentile.

As previously mentioned, the local emissions both from the neighbouring agglomeration and from the other aircraft — on tarmac and/or during the take-off/landing phases (in case the MOZAIC-IAGOS aircraft closely follows other aircraft) — may add some variability depending on the local dispersion conditions and thus influence the CO measurements in the LT. To assess more precisely the spatial representativeness of these MOZAIC-IAGOS LT data, some surface measurements are available at four German stations from the World Meteorology Organisation (WMO) Global Atmosphere Watch (GAW) database: Hohenpeissenberg (47.8°N, 11.0°W; at 50 km South-West from Munich), Neuglobsow (53.1°N, 13.0°W), Schauinsland (47.9°N, 7.9°W), Ochsenkopf site (50.0°N, 11.8°W). We investigate the correlations of both the seasonal and annual mean CO concentrations between the MOZAIC-IAGOS measurements (in the LT) and these surface observations (see Fig. S4 in the Supplement). At the annual scale, a reasonable agreement is found, with correlations (R) of annual mean CO between 0.56 (at Neuglobsow) and 0.81 (at Schauinsland). Considering the monthly time series, correlations are improved due to the seasonal variations (from 0.61 to 0.90). At the seasonal scale, correlations remain satisfactory in winter, with values between

0.65 and 0.87. However, results appear more contrasted among the GAW stations during the other seasons. In spring, all correlations are above 0.69 except Hohenpeissenberg (0.52). In summer, both Hohenpeissenberg and Ochsenkopf have a low correlation with MOZAIC-IAGOS (0.34 and 0.52, respectively), while very high correlations (above 0.96) are found for the two other stations. In autumn, the correlation is very low for Neuglobsow (-0.21), moderate for Ochsenkopf (0.51) and satisfactory for Hohenpeissenberg and Schauinsland (0.73 and 0.85).

Along the 2002-2012 period, the highest CO annual concentrations are encountered in 2003. This is in agreement with the satellite measurements that show on this year a high positive anomaly on CO total columns in Europe and more generally in North Hemisphere, notably due to intense boreal fires (Worden et al., 2013). High concentrations in the LT are also observed during the winter 2010, concomitantly with a cold snap over Europe that may have induced higher CO emissions (for the residential heating) (Cattiaux et al., 2010).

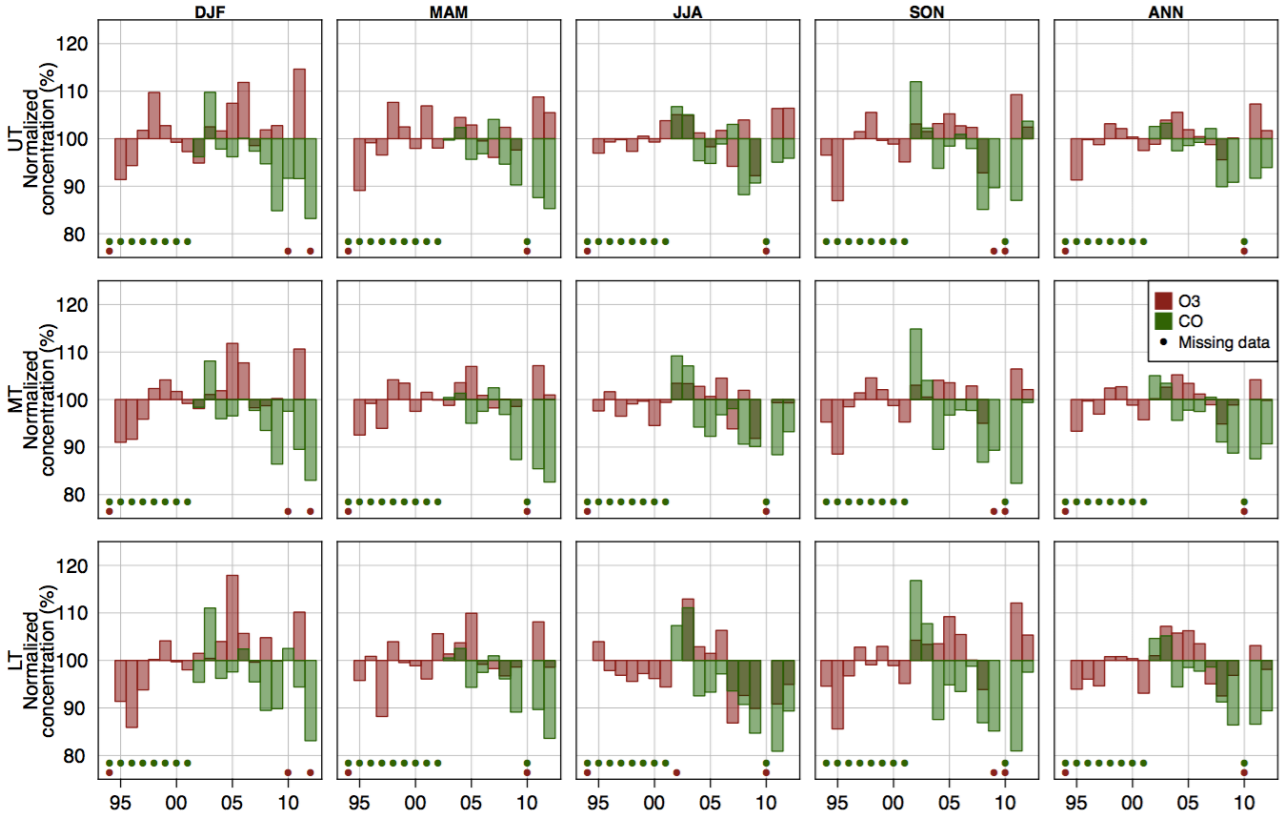

Figure 7: O_3 (in red) and CO (in green) seasonal and annual mean concentrations, normalized by the reference year (2000 for O_3, 2004 for CO) intercept obtained from the quadratic fit (see text), in the three tropospheric layers. Years and seasons with no data are indicated by dots.

3.3 Trends

In order to easily compare trends between the different tropospheric layers, O_3 concentrations are normalized following the approach of Parrish et al. (2014) : (i) a quadratic least-squares regression is applied to mean annual concentrations in which the year 2000 is taken as a reference (i.e. the origin of the time series), (ii) the obtained intercept corresponds to the interpolated mean annual O_3

concentration in 2000 (hereafter designated as $O_{3,2000}$), and is used for the normalization. Trends are thus expressed in percentage of year 2000 intercept per year (hereafter referred as $\%O_{3,2000}$ yr^{-1}). The same approach is used for each season. Considering the relatively short time coverage of MOZAIC-IAGOS observations (in comparison with measurements at some historical surface sites traditionally used for long-term trend calculations), we limit the analysis to linear regressions. Besides mean O_3 concentrations, we also investigate trends of the 5th and 95th percentiles. Hereafter, all these quantities are referred as $M(O_3)$, $P_5(O_3)$ and $P_{95}(O_3)$ for clarity. The same approach is followed for CO, with the year 2004 as a reference (and the results expressed in $\%CO_{2004}$ yr^{-1}). This year is chosen because in the three tropospheric layers, the mean CO concentrations in 2004 (140, 114 and 101 ppb in the LT, MT and UT, respectively) are very close to the mean CO concentrations over the 2002-2012 period (141, 114 and 102 ppb). Ozone and CO normalized mean concentrations at the annual and seasonal scale are shown in Fig. 7 (similar plots of the 5th and 95th percentile are given in Fig. S5-S6 in the Supplement).

Trends are investigated using the non-parametric Mann-Kendall analysis combined with Theil-Sen slope estimate (Sen, 1968) which has several important advantages compared to the least-square regression, including the absence of distributional assumptions and the lower sensitivity to outliers. We use the OpenAir package (in the statistical programming language R) developed for applications in atmospheric sciences (Carslaw and Ropkins, 2012). This package provides an estimation of the uncertainties based on the bootstrap method, and allows to take into account the autocorrelation of the data. The autocorrelation of environmental parameters is quite common (although often ignored in trend analysis), and tends to artificially decrease the uncertainties of trends, which can lead to the identification of trends that are actually insignificant (Weatherhead et al., 2002). Note that using our approach, the confidence intervals are not necessarily symmetric (around the mean slope estimate). The Theil-Sen slope estimates are reported in Table 1 (the corresponding absolute trends are reported in Table S1 in the Supplement). For information, the trend uncertainties obtained by ignoring the autocorrelation are reported in Table S2 in the Supplement.

Table 1: Annual and seasonal trends of mean O_3 and CO concentrations, 5th and 95th percentiles. Trends are estimated using the Theil-Sen slope estimate (see text). Uncertainties are given at the 95% confidence level (NS: non-significant trend). The significant O_3 trends over the 2000-2012 period are also reported in the footnotes below the Table.

		O_3 trend ($\%O_{3,2000}$ yr^{-1}) (1994-2012)			CO trend ($\%CO_{2004}$ yr^{-1}) (2002-2012)		
Season	Layer	Mean	5th	95th	Mean	5th	95th
Year	UT	NS	+0.63 [+0.09;+0.99]	NS	-1.36 [-2.05;-0.74]	-1.22 [-2.27;-0.47]	-1.43 [-2.08;-0.89]

			+0.42		-1.55	-1.57	-1.44
Year	MT	NS	[+0.09;+0.68]	NS	[-2.34;-0.72]	[-2.52;-0.68]	[-2.25;-0.59]
			+1.03		-1.51	-1.59	-1.41
Year	LT	NS	[+0.36;+1.62]	NS	[-2.42;-0.44]	[-2.58;-0.46]	[-2.40;-0.12]
		+0.62			-1.64	-1.39	-1.59
Winter	UT	[+0.02;+1.22][1]	NS	NS[3]	[-2.73;-0.80]	[-2.76;-0.39]	[-2.59;-1.06]
		+0.62			-1.50	-1.69	-1.22
Winter	MT	[+0.05;+1.22]	NS	NS	[-2.53;-0.60]	[-2.81;-0.31]	[-2.24;-0.28]
		+0.83					
Winter	LT	[+0.13;+1.67]	NS	NS	NS	NS	NS
					-1.67		-1.97
Spring	UT	NS	NS	NS	[-2.83;-0.48]	NS	[-3.13;-0.86]
					-2.00		-2.01
Spring	MT	NS	NS	NS	[-2.97;-0.69]	NS	[-2.71;-1.07]
					-1.91		-2.22
Spring	LT	NS	NS	NS	[-2.72;-1.09]	NS	[-4.04;-0.87]
							-1.53
Summer	UT	NS	NS	NS	NS	NS	[-2.22;-0.59]
					-1.83		-2.29
Summer	MT	NS	NS	NS	[-3.25;-0.56]	NS	[-3.77;-1.21]
					-2.31	-2.08	-2.63
Summer	LT	NS[2]	NS	NS	[-3.61;-0.97]	[-2.83;-0.76]	[-4.54;-1.42]
Autumn	UT	NS	NS	NS	NS	NS	NS
Autumn	MT	NS	NS	NS	NS	NS	NS
Autumn	LT	NS	NS	NS	NS	NS	NS

[1]: +1.08 [+0.29;+2.06]%$O_{3,2000}$ yr^{-1} over the 2000-2012 period.

[2]: -1.00 [-3.17;-0.02] %$O_{3,2000}$ yr^{-1}

[3]: +1.22 [+0.63;+2.27]%$O_{3,2000}$ yr^{-1}

3.3.1 Ozone

All the annual and seasonal trends of the $M(O_3)$ appear insignificant, except in winter for which a weakly significant increase is found in the three tropospheric layers (+0.83[+0.13;+1.67], +0.62[+0.05;+1.22] and +0.62[+0.02;+1.22]%$O_{3,2000}$ yr^{-1} in the LT, MT and UT, respectively). Concerning the $P_5(O_3)$, a significant increase is found at the annual scale in the three tropospheric layers (+1.03[+0.36;+1.62], +0.42[+0.09;+0.68] and +0.63[+0.09;+0.99]%$O_{3,2000}$ yr^{-1} in the LT, MT and UT, respectively). Conversely, trends of the $P_{95}(O_3)$ are all insignificant. Note that ignoring the autocorrelation of the data leads to some additional significant positive trends, including the $M(O_3)$ at the annual scale, the $P_5(O_3)$ in winter and autumn, and the $P_{95}(O_3)$ in winter, although not in all tropospheric layers (see Table S2 in the Supplement). It is beyond the scope of this study to

investigate why the autocorrelation has a stronger effect on these specific seasons or layers, but this illustrates the strong influence of the serial dependence on the trend analysis and the necessity to take it into account.

Most of the few positive trends found here over the whole period are due to an increase of O_3 in the 1990s. Over the 2000-2012 period, the only persistent significant trend among the previous ones is the increase of the $M(O_3)$ in the UT during winter (+1.08[+0.29;+2.06]%$O_{3,2000}$ yr^{-1}). However, interestingly, a few other trends become significant over that period, including the decrease of the $M(O_3)$ in the LT during the summer (-1.00[-3.17;-0.02] %$O_{3,2000}$ yr^{-1}), and the increase of the $P_{95}(O_3)$ in the UT during the winter (+1.22[+0.63;+2.27]%$O_{3,2000}$ yr^{-1}). Previous trend analysis at the alpine sites (Zugspitze since 1978, Jungfraujoch and Sonnblick since 1990) have highlighted (i) a strong increase of O_3 during all seasons in the 1980s (around 0.6-0.9 ppb yr^{-1}), (ii) a persistent but lower increase in the 1990s during all seasons except summer where O_3 has levelled off, (iii) the extension of that levelling off in the 2000s to the other seasons and a slight decrease in summer (Logan et al., 2012; Parrish et al., 2012). Qualitatively, this picture is in general agreement with our results in the lower part of the troposphere (e.g. significant increase in winter, negative trend in summer for 2000-2012). Interestingly, at regional background sites in Europe over the 2-3 last decades, Parrish et al. (2012) highlighted that O_3 trends, when they are expressed relatively to the concentration in 2000, are quite similar (around +1% $O_{3,2000}$ yr^{-1}) whatever the site and the season. Although not directly comparable due to a different (and shorter) time period, our study shows that the increase of wintertime O_3 over the 1994-2012 period is slightly lower but differences remain insignificant. At low altitudes, this increase of O_3 in winter has been observed at several sites in Europe and North America (Cooper et al., 2012; Derwent et al., 2013; Wilson et al., 2012) and is mainly attributed to a reduced O_3 titration by NO due to decreasing NO_x emissions (e.g. Ordóñez et al., 2005). The persistent positive trends found higher in altitude suggest that wintertime O_3 has increased at a large scale (if not hemispheric) (see Fig. 2). Based on the MOZAIC dataset at Frankfurt/Munich over the 1995-2008 period, at about 3 km, Logan et al. (2012) highlighted a significant increase of O_3 concentrations in winter (around +0.5±0.2 ppb yr^{-1}) and to a lesser extent in spring (around +0.25±0.2 ppb yr^{-1}), and insignificant trends during the other seasons. At the annual scale, the trend is around +0.2 ppb yr^{-1} up to 4 km and +0.4-0.6 ppb yr^{-1} between 4 and 8 km. Over the same period and using the same statistical approach (i.e. multiple linear regression of the annual cycle and the four seasonal trends from the monthly time series), we also found in the MT an increase in winter and spring, as well as at the annual scale in all tropospheric layers. However, our trends in the MT and UT (+0.19±0.10 and +0.17±0.13 ppb yr^{-1}, respectively, as calculated with the Logan's approach) are lower than those reported by Logan et al. (2012) (although differences do not appear to be significant). This is likely due to the fact that only the troposphere is considered in this present study.

3.3.2 Carbon monoxide

As previously mentioned, CO trends are here investigated relatively to the 2004 reference year. Over the 2002-2012 period, the M(CO) at the annual scale significantly decreases in the whole troposphere, with trends of -1.51[-2.42;-0.44], -1.55[-2.34;-0.72] and -1.36[-2.05;-0.74]%CO_{2004} yr^{-1} in the LT, MT and UT, respectively. Similar negative trends are also obtained for the P_5(CO) and P_{95}(CO) in all the tropospheric layers. At the seasonal scale, the M(CO) and P_{95}(CO) show negative trends in winter, spring and summer, although not always in all the tropospheric layers, while the P_5(CO) is decreasing only in winter (in the MT and UT) and summer (only in the LT). Conversely, all trends in autumn are insignificant. Note that the results without taking into consideration the autocorrelation of the data show significant negative trends of the P_5(CO) in most layers and during all the seasons, except autumn (see Table S2 in the Supplement). These results are in general agreement with previous studies in Europe (e.g., Karlsdóttir et al., 2000; Novelli et al., 2003; Dils et al., 2009; Worden et al., 2013). Based on satellite observations, Worden et al. (2013) highlighted over Europe a decrease of the CO total columns, around -1.44+0.22% yr^{-1} with MOPITT over 2001-2011 and -1.00±0.33% yr^{-1} with AIRS over 2003-2011, thus in the range of our results over Frankfurt. Over the 1995-2007 period, Gilge et al. (2010) found trends of -3.36±1.08 and -1.51±0.64 ppb yr^{-1} (reduced to -2.65±0.04 ppb yr^{-1} by filtering the background values (Zellweger et al., 2009)) at two alpine sites from the WMO GAW network, in reasonable agreement with our absolute Theil-Sen slope estimates at Frankfurt/Munich in the LT and MT (-2.24[-3.59;-0.65] and -1.85[-2.79;-0.85] ppb yr^{-1}).

3.4 Changes of the O_3 seasonal cycle

In the previous section, we highlighted differences in the O_3 trends depending on the season and the tropospheric layer. Here, we investigate if these contrasted trends come along a change of the O_3 seasonal cycle above Frankfurt/Munich (Sect. 3.4.1). Results are discussed in Sect. 3.4.2.

3.4.1 Evolution of the seasonal cycle at Frankfurt/Munich

The seasonal variation of O_3 can be well approximated by a sine function fully characterized by three parameters: an offset value defined here as the average O_3 concentration over the considered period, an amplitude, and a phase that determines at which period in the year the maximum of O_3 is reached. Following Parrish et al. (2013), one can fit a sine function to the monthly time series over a period of several years:

$$\tilde{y}(t) = y_0 + a \sin\left(\frac{2\pi t}{12} + \phi\right) \quad (1)$$

with t the time (in months, values ranging between 1 and 12), y_0 the offset concentration (in ppb), a the amplitude (in ppb) and ϕ the phase. For clarity, one can consider ϕ_{month} defined as:

$$\phi_{month} = \frac{12}{2\pi}\left(\frac{\pi}{2} - \phi\right) \quad (2)$$

that now corresponds to the decimal month of maximum O_3 (for instance, values of 1 and 6.5 correspond to a maximum of the fitted O_3 occurring the 1st January and the 15th June, respectively).

Results are presented in Fig. 7 for moving 9-year time periods. The width of this window is chosen in order to avoid any overlap between the first (1995-2003) and the last (2003-2012) time period, which allows to compare the results from independent datasets. It is worth noting that the dates of maximum O_3 obtained here (for instance, the 28 May in the LT and the 6-7 June in the MT and UT, over the 1995-2003 period) do not exactly correspond to those given by the averaged seasonal variations, in particular in the MT and UT where O_3 is maximum in July (see Fig. 4). This is due to the fact that the O_3 seasonal pattern does not follow exactly a sinusoid. For instance, in the UT, the July maximum is driven by several high episodes during this month (with a high interannual variability). However, compared to the rest of the year, the weight of this July month is minor and thus it does not influence so much the fitted sinusoid that gives a maximum earlier in the year. This can be clearly demonstrated by fitting a sinusoid on the averaged seasonal profiles shown in Fig. 4, which for instance gives a ϕ_{month} of 6.2 in the UT (see Fig. S7 in the Supplement). In addition, this is not so problematic since we are here more interested in the relative changes of the seasonal pattern than in the seasonal pattern itself.

For each point (that corresponds to a 9-year time period), the 95% confidence level is derived from the linear regression for both the amplitude and the phase, and represented by a coloured area on Fig. 7. These uncertainties need to be taken into account in order to fully quantify the trend and its corresponding uncertainty. Instead of using a simple linear regression, we thus follow the procedure precisely described in the numerical recipes of Press et al. (2007) (see equations 15.2.4 to 15.2.12) in which all uncertainties are considered in the calculation of the trend, its uncertainty and its goodness-of-fit (following Press et al. (2007), we consider the derived linear model as believable only when the goodness-of-fit exceeds 0.1). Note that the trends obtained with this procedure are always very close to those derived from a simple linear regression, but their uncertainties are substantially higher (up to a factor of 2-3 higher). We focus here on the changes of amplitude and phase.

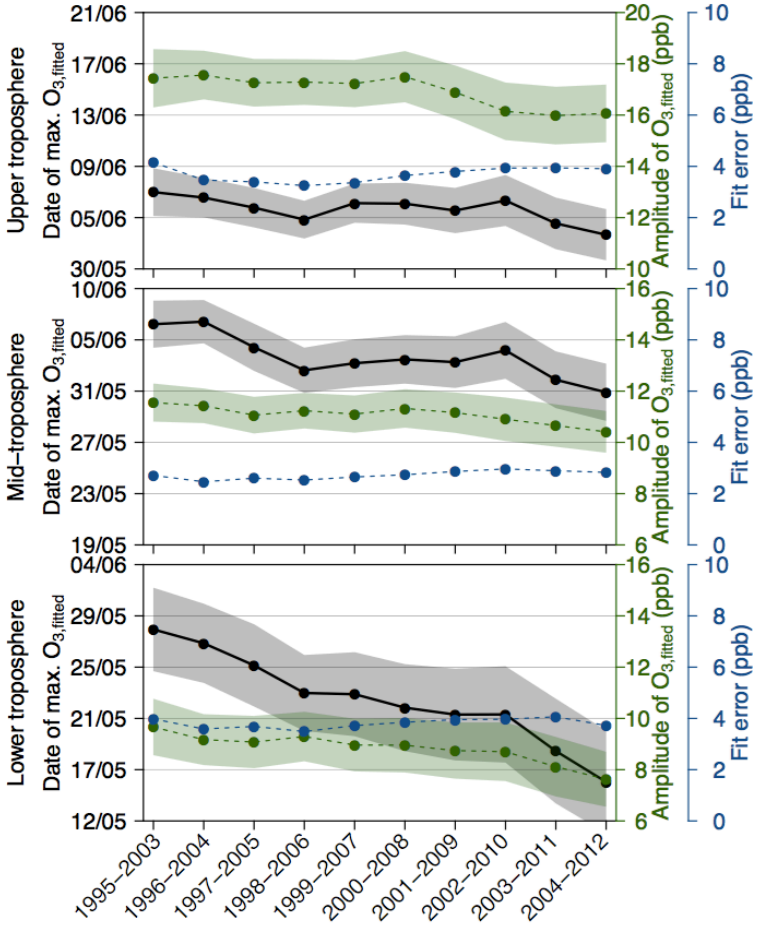

Figure 7: Date of maximum (in black) and amplitude (in green) of the fitted O_3 seasonal cycle (referred as $O_{3,fitted}$), and error of the fit (in blue) on moving periods of 9 years (see text for more details on the procedure). For the two first parameters, 95% confidence intervals are indicated. Layers: UT (top), MT (middle), LT (bottom). Note that the same scale (but different offsets) is used in all layers, so that trends and confidence intervals are thus directly comparable.

Results show a decrease around 1-2 ppb of the amplitude of the O_3 seasonal cycle in the three tropospheric layers along the 1995-2012 period. Between the first (1995-2003) and the last 9-year period (2004-2012), trends are -1.8±1.2, -1.0±0.8 and -1.8±1.2 ppb decade^{-1} in the LT, MT and UT, respectively (-20.0±13.4, -8.8±7.6 and -10.6±7.0% decade^{-1} in relative). This is consistent with the fact that O_3 has increased significantly in the whole troposphere during the winter (the season of minimum O_3) but not during spring/summer (the season of maximum O_3) (see Sect. 3.3.1).

Concerning the phase of the O_3 seasonal cycle, results clearly highlight a shift toward earlier O_3 maximum along the 1995-2012 period. This shift is the strongest in the LT (-12.1±4.1 days decade^{-1}), substantially lower in the MT (-5.2±2.3 days decade^{-1}) and reaches its minimum in the UT (-2.3±2.1 days decade^{-1}). It thus significantly decreases with the altitude (i.e., differences between all these trends are statistically significant). Note that applying the same procedure to the $P_5(O_3)$ also leads to significant seasonal shifts (-11.1±6.1, -16.0±6.0 and -6.2±4.7 days decade^{-1} in the LT, MT

and UT, respectively). Conversely, the seasonal shift of the $P_{95}(O_3)$ is much lower and significant only in the LT (-8.0±4.0 days decade^{-1}).

A similar analysis has been done on some O_3 surface measurements (GAW database; 12 sites) in Europe during the 1995-2012 period (see Sect. S.1 in the Supplement). At the surface, except at one remote site in Sweden, all sites show a shift of the seasonal cycle in the same direction than obtained at Frankfurt/Munich, i.e., toward an earlier O_3 maximum. However, results appear very contrasted with shifts ranging from -15.1±3.0 to -3.9±3.9 days decade^{-1}, without any clear relation with the type of site (coastal, mountain, continental), the altitude or the level of O_3 concentration. In comparison, Parrish et al. (2013) have reported at four ground sites in Europe (two alpine sites including Jungfraujoch, the low elevation Hohenpeissenberg site and the Mace Head coastal site) shifts of the O_3 seasonal cycle in the same direction (i.e., toward earlier O_3 maximum), but with lower rates than found here in the LT. At the three continental sites, rates of shift were statistically significant at the 95% confidence level and ranged between -5 and -7 days decade^{-1} since 1970s. At the Mace Head coastal site, the rate was lower and insignificant (-3±3.7 days decade^{-1}). Discrepancies are likely due to the fact that the studied periods are different. As a faster change of phase is found between 2005 and 2008 (their 3 last years) (see Fig. 2 in Parrish et al. (2013)), restricting their analysis to our shorter period would likely lead to a higher seasonal shift (i.e., closer to our values). Over the 1995-2012 period, the same analysis performed at three ozonesonde sites in Europe (NDACC database) also shows a shift toward earlier O_3 maxima (see Sect. S.1 in the Supplement). Interestingly, in agreement with our results at Frankfurt/Munich, the shifts tend to be stronger close to the surface than at higher levels, up to a positive shift at the highest altitudes at one site. For instance, the shifts at the Uccle (Hohenpeissenberg) site are -17.5±7.0, -11.5±4.6, +1.4±4.1 and +7.2±6.5 days decade^{-1} (-7.5±4.2, -9.0±3.6, -4.2±2.7 and -1.7±6.2 days decade^{-1}) at 900-800, 800-600, 600-400 and 400-300 hPa, respectively. This feature is even clearer when calculations are performed over the whole period of available data.

3.4.2 Discussion

This study confirms that the ozone seasonal pattern in Central/Western Europe is changing, at least since the mid-1990s, moving toward a lower amplitude and an earlier O_3 maximum (Sect. 3.4). Thanks to vertical profile observations, it brings an interesting contribution by highlighting that these seasonal changes above Frankfurt/Munich depend on altitude, with the highest shift in the LT and much lower ones in the UT and to a lesser extent in the MT. It is worth noting that the MOZAIC-IAGOS observations above Frankfurt/Munich represent the densest dataset of O_3 vertical profiles in the world, which gives robustness to our results. Qualitatively, a similar behaviour is observed in ozonesonde observations but the reliability of these results is limited by a much lower number of vertical profiles. However, a high variability from one site to the other in Europe affects

both the rate of decrease with altitude and the shift extent itself, as confirmed by results obtained at surface stations.

Parrish et al. (2013) exhaustively discussed several reasons that may explain this changing phase at surface in Europe, including changes in downward transport of stratospheric O_3, long-range transport, O_3 precursor's emissions and their spatial distribution, photochemical production and the potential influence of climate change. Our study does not provide an unambiguous explanation to either the seasonal trends discrepancies or the subsequent seasonal shifts (which would ideally require the use of global models able to correctly reproduce both O_3 seasonal patterns and trends throughout the troposphere). In terms of stratospheric contributions, stratosphere-to-troposphere (STT) ozone fluxes are known to peak in spring (Auvray and Bey, 2005; James et al., 2003; Tang et al., 2011) due to both enhanced downward transport and maximum concentrations in the lowermost stratosphere (e.g., Thouret et al., 2006). If the seasonal shift was induced by higher STT fluxes, one would expect stronger positive trends in spring and a similar (and even stronger) shift close to the tropopause compared to the LT, which is contradicted by our observations. Thus, the exchanges between the stratosphere and the troposphere are not likely the main reason explaining the shift of the O_3 seasonal pattern. The trend analysis (Sect. 3.3) has not highlighted any significant O_3 trend either in spring or summer, the large uncertainties being at least partly due to the strong interannual variability of O_3 concentrations. However, one can qualitatively notice on Fig. 7 that over our period, the O_3 anomalies in summer tend to be more and more negative in the LT, contrary to the UT where they tend to be slightly positive at the end of the period. This is probably mainly due to the decrease of O_3 precursors emissions in Europe (Derwent et al., 2003; Solberg et al., 2005; Jonson et al., 2006). As there are no such differences of O_3 anomalies between the tropospheric layers during the spring, this may at least partly explain the higher seasonal shift found close to the surface.

4 Summary and conclusions

An extensive database of O_3 and CO vertical profiles above worldwide airports is available from the MOZAIC-IAGOS program since 1994 and 2002, respectively. In this study, we investigate the climatology, variations and trends of O_3 and CO concentrations above the Frankfurt and Munich airports whose combination represents the densest and longest MOZAIC-IAGOS dataset. We focus on the troposphere, each vertical profile being subdivided in three tropospheric layers — the lower, mid- and upper troposphere (LT, MT and UT, respectively) — based on the potential vorticity extracted from ECMWF meteorological data. Main results are given below (all trends are given with uncertainties at a 95% confidence level):

1. Climatological vertical profiles: The mean O_3 vertical profile is characterized by a strong increase with altitude in the first kilometre above the surface whatever the season and close

to the tropopause in spring/summer, while the gradient remains moderate (low) in the free troposphere in spring/summer (winter/autumn). These variations of the O_3 vertical gradient are likely due to the effect of deposition and titration by NO close to the surface, and stratosphere-to-troposphere exchanges close to the tropopause. We also highlighted a minimum of daily O_3 variability at around 3-4 km. The mean CO vertical profile shows maximum concentrations at the surface, a strong decrease in the first kilometre (in particular in winter/autumn) and a moderate one in the rest of the troposphere. A maximum of variability is also found at the surface, while that variability remains constant (around 18%) through the rest of the troposphere, whatever the season.

2. Seasonal variations: The mean O_3 seasonal variations show a minimum in November-December in all tropospheric layers, a broad spring/summer maximum in the LT and MT and a sharper summer maximum in the UT. The O_3 5^{th} percentile is also minimum in November-December in all the troposphere, but reaches its maximum in April-May in the LT and MT, and April-August in the UT. The seasonal profile of the O_3 95^{th} percentile is less contrasted in the troposphere, with a maximum in April-August in the LT, July-August in the MT and May-July in the UT. The mean CO seasonal variations peak in March/April in the whole troposphere, and reach a broad minimum in July-October in the LT, refined to September/October in the MT and UT. A quite similar pattern is observed for the CO 5^{th} and 95^{th} percentiles.
3. Annual and seasonal O_3 trends: Over the 1994-2012 period, most O_3 trends are insignificant. The few exceptions are the significant increases of the mean O3 in winter, and the O_3 5^{th} percentile at the annual scale. No significant trends are found for the O_3 95^{th} percentile. Considering the uncertainties at a 95% confidence level, the significant trend values range between 0.02 and 1.67%$O_{3,2000}$ yr^{-1} (relative change with the year 2000 as a reference). This increase occurred mainly during the 1990s, as only the increase of the mean O_3 during the winter in the UT persists when the analysis is restricted to the 2000-2012 period. However, over that period, results show a significant decrease of the mean O_3 during the summer in the LT, as well as an increase of the O_3 95^{th} percentile during the winter in the UT.
4. Annual and seasonal CO trends: Over the 2002-2012 period, the mean CO concentrations are decreasing at the annual scale and at the seasonal scale in winter, spring and summer in all the tropospheric layers (except in the LT in winter), with trends ranging between -2.31[-3.61;-0.97] and -1.36[-2.05;-0.74]%CO_{2004} yr^{-1} (relative change with the year 2004 as a reference). A similar picture is observed for both the 5^{th} and the 95^{th} percentiles, except that most trends in spring and summer are insignificant for the 5^{th} percentile. All trends remain insignificant in autumn.

This study also investigates the changes in the O_3 seasonal cycle (by fitting sinusoids over 9-years moving time periods) with a focus on the phase. Results highlight a statistically significant change of the phase in the LT, ozone maxima occurring earlier by -12.1±4.1 days decade^{-1} on average (at a 95% confidence level), in general agreement with previous results from the literature (Parrish et al., 2013). Observations at most surface stations in Central Europe show seasonal shifts in the same direction (toward earlier maxima), but with a strong variability from one station to the other. A major contribution of this study concerns the dependence on altitude of this seasonal shift, as it is found to decrease by a factor of two in the mid-troposphere (-5.2±2.3 days decade^{-1}) and five in the upper troposphere (-2.3±2.1 days decade^{-1}). Qualitatively, a similar dependence on altitude is obtained with ozonesonde observations at most sites in Europe. The occurrence of negative O_3 anomalies during the summer in the LT but not in the other layers, probably induced by the reduction of O_3 precursors emissions in Europe, may at least partly explain the higher seasonal shift observed at low altitudes. The larger contribution from other regions (e.g. Asia) higher in altitude may explain the lower seasonal shift observed in the UT, although further studies are obviously required to quantitatively assess this issue.

References

Ashmore, M. R.: Assessing the future global impacts of ozone on vegetation, Plant, Cell Environ., 28(8), 949–964, doi:10.1111/j.1365-3040.2005.01341.x, 2005.

Auvray, M. and Bey, I.: Long-range transport to Europe: Seasonal variations and implications for the European ozone budget, J. Geophys. Res., 110(D11), D11303, doi:10.1029/2004JD005503, 2005.

Bethan, S., Vaughan, G. and Reid, S. J.: A comparison of ozone and thermal tropopause heights and the impact of tropopause definition on quantifying the ozone content of the troposphere, Q. J. R. Meteorol. Soc., 122(532), 929–944, doi:10.1002/qj.49712253207, 1996.

Carslaw, D. C. and Ropkins, K.: openair — An R package for air quality data analysis, Environ. Model. Softw., 27-28, 52–61, doi:10.1016/j.envsoft.2011.09.008, 2012.

Cattiaux, J., Vautard, R., Cassou, C., Yiou, P., Masson-Delmotte, V. and Codron, F.: Winter 2010 in Europe: A cold extreme in a warming climate, Geophys. Res. Lett., 37(20), n/a–n/a, doi:10.1029/2010GL044613, 2010.

Chevalier, A., Gheusi, F., Delmas, R., Ordóñez, C., Sarrat, C., Zbinden, R., Thouret, V., Athier, G. and Cousin, J.-M.: Influence of altitude on ozone levels and variability in the lower troposphere: a ground-based study for western Europe over the period 2001–2004, Atmos. Chem. Phys., 7(16), 4311–4326, doi:10.5194/acp-7-4311-2007, 2007.

Cooper, O. R., Gao, R.-S., Tarasick, D., Leblanc, T. and Sweeney, C.: Long-term ozone trends at rural ozone monitoring sites across the United States, 1990-2010, J. Geophys. Res. Atmos.,

117(D22), n/a–n/a, doi:10.1029/2012JD018261, 2012.
Cooper, O. R., Parrish, D. D., Ziemke, J., Balashov, N. V., Cupeiro, M., Galbally, I. E., Gilge, S., Horowitz, L., Jensen, N. R., Lamarque, J.-F., Naik, V., Oltmans, S. J., Schwab, J., Shindell, D. T., Thompson, A. M., Thouret, V., Wang, Y. and Zbinden, R. M.: Global distribution and trends of tropospheric ozone: An observation-based review, Elem. Sci. Anthr., 2, 000029, doi:10.12952/journal.elementa.000029, 2014.
Cui, J., Pandey Deolal, S., Sprenger, M., Henne, S., Staehelin, J., Steinbacher, M. and Nédélec, P.: Free tropospheric ozone changes over Europe as observed at Jungfraujoch (1990–2008): An analysis based on backward trajectories, J. Geophys. Res., 116(D10), D10304, doi:10.1029/2010JD015154, 2011.
Derwent, R. ., Jenkin, M. ., Saunders, S. ., Pilling, M. ., Simmonds, P. ., Passant, N. ., Dollard, G. ., Dumitrean, P. and Kent, A.: Photochemical ozone formation in north west Europe and its control, Atmos. Environ., 37(14), 1983–1991, doi:10.1016/S1352-2310(03)00031-1, 2003.
Derwent, R. G., Manning, A. J., Simmonds, P. G., Spain, T. G. and O'Doherty, S.: Analysis and interpretation of 25 years of ozone observations at the Mace Head Atmospheric Research Station on the Atlantic Ocean coast of Ireland from 1987 to 2012, Atmos. Environ., 80, 361–368, doi:10.1016/j.atmosenv.2013.08.003, 2013.
Van Dingenen, R., Dentener, F. J., Raes, F., Krol, M. C., Emberson, L. and Cofala, J.: The global impact of ozone on agricultural crop yields under current and future air quality legislation, Atmos. Environ., 43(3), 604–618, doi:10.1016/j.atmosenv.2008.10.033, 2009.
Gaudel, A., Ancellet, G. and Godin-Beekmann, S.: Analysis of 20 years of tropospheric ozone vertical profiles by lidar and ECC at Observatoire de Haute Provence (OHP) at 44°N, 6.7°E, Atmos. Environ., 113, 78–89, doi:10.1016/j.atmosenv.2015.04.028, 2015.
Gilge, S., Plass-Duelmer, C., Fricke, W., Kaiser, A., Ries, L., Buchmann, B. and Steinbacher, M.: Ozone, carbon monoxide and nitrogen oxides time series at four alpine GAW mountain stations in central Europe, Atmos. Chem. Phys., 10(24), 12295–12316, doi:10.5194/acp-10-12295-2010, 2010.
Holloway, T., Levy, H. and Kasibhatla, P.: Global distribution of carbon monoxide, J. Geophys. Res., 105(D10), 12123, doi:10.1029/1999JD901173, 2000.
IPCC: Climate change 2013 : The physical science basis. [online] Available from: http://www.ipcc.ch/report/ar5/wg1/, 2013.
James, P., Stohl, A., Forster, C., Eckhardt, S., Seibert, P. and Frank, A.: A 15-year climatology of stratosphere-troposphere exchange with a Lagrangian particle dispersion model: 1. Methodology and validation, J. Geophys. Res., 108(D12), 8519, doi:10.1029/2002JD002637, 2003.
Jerrett, M., Burnett, R. T., Pope, C. A., Ito, K., Thurston, G., Krewski, D., Shi, Y., Calle, E. and Thun, M.: Long-term ozone exposure and mortality., N. Engl. J. Med., 360(11), 1085–95, doi:10.1056/NEJMoa0803894, 2009.

Jonson, J. E., Simpson, D., Fagerli, H. and Solberg, S.: Can we explain the trends in European ozone levels?, Atmos. Chem. Phys., 6(1), 51–66, doi:10.5194/acp-6-51-2006, 2006.

Junge, C. E.: Residence time and variability of tropospheric trace gases, Tellus, 26(4), 477–488, doi:10.1111/j.2153-3490.1974.tb01625.x, 1974.

Karlsdóttir, S., Isaksen, I. S. A., Myhre, G. and Berntsen, T. K.: Trend analysis of O 3 and CO in the period 1980–1996: A three-dimensional model study, J. Geophys. Res., 105(D23), 28907, doi:10.1029/2000JD900374, 2000.

Koumoutsaris, S., Bey, I., Generoso, S. and Thouret, V.: Influence of El Niño–Southern Oscillation on the interannual variability of tropospheric ozone in the northern midlatitudes, J. Geophys. Res., 113(D19), D19301, doi:10.1029/2007JD009753, 2008.

Kunz, A., Konopka, P., Müller, R. and Pan, L. L.: Dynamical tropopause based on isentropic potential vorticity gradients, J. Geophys. Res., 116(D1), D01110, doi:10.1029/2010JD014343, 2011.

Logan, J. A., Megretskaia, I. A., Miller, A. J., Tiao, G. C., Choi, D., Zhang, L., Stolarski, R. S., Labow, G. J., Hollandsworth, S. M., Bodeker, G. E., Claude, H., De Muer, D., Kerr, J. B., Tarasick, D. W., Oltmans, S. J., Johnson, B., Schmidlin, F., Staehelin, J., Viatte, P. and Uchino, O.: Trends in the vertical distribution of ozone: A comparison of two analyses of ozonesonde data, J. Geophys. Res., 104(D21), 26373, doi:10.1029/1999JD900300, 1999.

Logan, J. A., Staehelin, J., Megretskaia, I. A., Cammas, J.-P., Thouret, V., Claude, H., De Backer, H., Steinbacher, M., Scheel, H.-E., Stübi, R., Fröhlich, M. and Derwent, R.: Changes in ozone over Europe: Analysis of ozone measurements from sondes, regular aircraft (MOZAIC) and alpine surface sites, J. Geophys. Res., 117(D9), D09301, doi:10.1029/2011JD016952, 2012.

Moise, T. and Rudich, Y.: Reactive uptake of ozone by proxies for organic aerosols: Surface versus bulk processes, J. Geophys. Res., 105(D11), 14667, doi:10.1029/2000JD900071, 2000.

Moise, T. and Rudich, Y.: Reactive Uptake of Ozone by Aerosol-Associated Unsaturated Fatty Acids: Kinetics, Mechanism, and Products, J. Phys. Chem. A, 106(27), 6469–6476, doi:10.1021/jp025597e, 2002.

Nedelec, P., Cammas, J.-P., Thouret, V., Athier, G., Cousin, J.-M., Legrand, C., Abonnel, C., Lecoeur, F., Cayez, G. and Marizy, C.: An improved infrared carbon monoxide analyser for routine measurements aboard commercial Airbus aircraft: technical validation and first scientific results of the MOZAIC III programme, Atmos. Chem. Phys., 3(5), 1551–1564, doi:10.5194/acp-3-1551-2003, 2003.

Nédélec, P., Blot, R., Boulanger, D., Athier, G., Cousin, J.-M., Gautron, B., Petzold, A., Volz-Thomas, A. and Thouret, V.: Instrumentation on commercial aircraft for monitoring the atmospheric composition on a global scale: the IAGOS system, technical overview of ozone and carbon monoxide measurements, Tellus B, 67, doi:10.3402/tellusb.v67.27791, 2015.

Novelli, P. C., Masarie, K. A., Lang, P. M., Hall, B. D., Myers, R. C. and Elkins, J. W.: Reanalysis of tropospheric CO trends: Effects of the 1997–1998 wildfires, J. Geophys. Res., 108(D15), 4464, doi:10.1029/2002JD003031, 2003.

Oltmans, S. J., Lefohn, A. S., Scheel, H. E., Harris, J. M., Levy, H., Galbally, I. E., Brunke, E.-G., Meyer, C. P., Lathrop, J. A., Johnson, B. J., Shadwick, D. S., Cuevas, E., Schmidlin, F. J., Tarasick, D. W., Claude, H., Kerr, J. B., Uchino, O. and Mohnen, V.: Trends of ozone in the troposphere, Geophys. Res. Lett., 25(2), 139–142, doi:10.1029/97GL03505, 1998.

Oltmans, S. J., Lefohn, A. S., Harris, J. M., Galbally, I., Scheel, H. E., Bodeker, G., Brunke, E., Claude, H., Tarasick, D., Johnson, B. J., Simmonds, P., Shadwick, D., Anlauf, K., Hayden, K., Schmidlin, F., Fujimoto, T., Akagi, K., Meyer, C., Nichol, S., Davies, J., Redondas, A. and Cuevas, E.: Long-term changes in tropospheric ozone, Atmos. Environ., 40(17), 3156–3173, doi:10.1016/j.atmosenv.2006.01.029, 2006.

Oltmans, S. J., Lefohn, A. S., Shadwick, D., Harris, J. M., Scheel, H. E., Galbally, I., Tarasick, D. W., Johnson, B. J., Brunke, E.-G., Claude, H., Zeng, G., Nichol, S., Schmidlin, F., Davies, J., Cuevas, E., Redondas, A., Naoe, H., Nakano, T. and Kawasato, T.: Recent tropospheric ozone changes – A pattern dominated by slow or no growth, Atmos. Environ., 67, 331–351, doi:10.1016/j.atmosenv.2012.10.057, 2013.

Ordóñez, C., Mathis, H., Furger, M., Henne, S., Hüglin, C., Staehelin, J. and Prévôt, A. S. H.: Changes of daily surface ozone maxima in Switzerland in all seasons from 1992 to 2002 and discussion of summer 2003, Atmos. Chem. Phys., 5(5), 1187–1203, doi:10.5194/acp-5-1187-2005, 2005.

Ordóñez, C., Brunner, D., Staehelin, J., Hadjinicolaou, P., Pyle, J. A., Jonas, M., Wernli, H. and Prévôt, A. S. H.: Strong influence of lowermost stratospheric ozone on lower tropospheric background ozone changes over Europe, Geophys. Res. Lett., 34(7), L07805, doi:10.1029/2006GL029113, 2007.

Paoletti, E.: Impact of ozone on Mediterranean forests: a review., Environ. Pollut., 144(2), 463–74, doi:10.1016/j.envpol.2005.12.051, 2006.

Parrish, D. D., Law, K. S., Staehelin, J., Derwent, R., Cooper, O. R., Tanimoto, H., Volz-Thomas, A., Gilge, S., Scheel, H.-E., Steinbacher, M. and Chan, E.: Long-term changes in lower tropospheric baseline ozone concentrations at northern mid-latitudes, Atmos. Chem. Phys., 12(23), 11485–11504, doi:10.5194/acp-12-11485-2012, 2012.

Parrish, D. D., Law, K. S., Staehelin, J., Derwent, R., Cooper, O. R., Tanimoto, H., Volz-Thomas, A., Gilge, S., Scheel, H.-E., Steinbacher, M. and Chan, E.: Lower tropospheric ozone at northern midlatitudes: Changing seasonal cycle, Geophys. Res. Lett., 40(8), 1631–1636, doi:10.1002/grl.50303, 2013.

Parrish, D. D., Lamarque, J.-F., Naik, V., Horowitz, L., Shindell, D. T., Staehelin, J., Derwent, R.,

Cooper, O. R., Tanimoto, H., Volz-Thomas, A., Gilge, S., Scheel, H.-E., Steinbacher, M. and Fröhlich, M.: Long-term changes in lower tropospheric baseline ozone concentrations: Comparing chemistry-climate models and observations at northern midlatitudes, J. Geophys. Res. Atmos., 119(9), 5719–5736, doi:10.1002/2013JD021435, 2014.

Petzold, A., Thouret, V., Gerbig, C., Zahn, A., Brenninkmeijer, C. A. M., Gallagher, M., Hermann, M., Pontaud, M., Ziereis, H., Boulanger, D., Marshall, J., Nédélec, P., Smit, H. G. J., Friess, U., Flaud, J.-M., Wahner, A., Cammas, J.-P. and Volz-Thomas, A.: Global-scale atmosphere monitoring by in-service aircraft – current achievements and future prospects of the European Research Infrastructure IAGOS, Tellus B, 67, doi:10.3402/tellusb.v67.28452, 2015.

Press, W. H., Teukolsky, S. A., Vetterling, W. T. and Flannery, B. P.: Numerical Recipies: The Art of Scientific Computing, 3rd Edition, Cambridge ., 2007.

Sen, P. K.: Estimates of the Regression Coefficient Based on Kendall's Tau, J. Am. Stat. Assoc., 63(324), 1379–1389, doi:10.1080/01621459.1968.10480934, 1968.

Simmonds, P. G., Derwent, R. G., Manning, A. L. and Spain, G.: Significant growth in surface ozone at Mace Head, Ireland, 1987–2003, Atmos. Environ., 38(28), 4769–4778, doi:10.1016/j.atmosenv.2004.04.036, 2004.

Solberg, S., Bergström, R., Langner, J., Laurila, T. and Lindskog, A.: Changes in Nordic surface ozone episodes due to European emission reductions in the 1990s, Atmos. Environ., 39(1), 179–192, doi:10.1016/j.atmosenv.2004.08.049, 2005.

Solberg, S., Hov, Ø., Søvde, A., Isaksen, I. S. A., Coddeville, P., De Backer, H., Forster, C., Orsolini, Y. and Uhse, K.: European surface ozone in the extreme summer 2003, J. Geophys. Res., 113(D7), D07307, doi:10.1029/2007JD009098, 2008.

Staufer, J., Staehelin, J., Stübi, R., Peter, T., Tummon, F. and Thouret, V.: Trajectory matching of ozonesondes and MOZAIC measurements in the UTLS – Part 1: Method description and application at Payerne, Switzerland, Atmos. Meas. Tech., 6(12), 3393–3406, doi:10.5194/amt-6-3393-2013, 2013.

Staufer, J., Staehelin, J., Stübi, R., Peter, T., Tummon, F. and Thouret, V.: Trajectory matching of ozonesondes and MOZAIC measurements in the UTLS – Part 2: Application to the global ozonesonde network, Atmos. Meas. Tech., 7(1), 241–266, doi:10.5194/amt-7-241-2014, 2014.

Stevenson, D. S., Dentener, F. J., Schultz, M. G., Ellingsen, K., van Noije, T. P. C., Wild, O., Zeng, G., Amann, M., Atherton, C. S., Bell, N., Bergmann, D. J., Bey, I., Butler, T., Cofala, J., Collins, W. J., Derwent, R. G., Doherty, R. M., Drevet, J., Eskes, H. J., Fiore, A. M., Gauss, M., Hauglustaine, D. A., Horowitz, L. W., Isaksen, I. S. A., Krol, M. C., Lamarque, J.-F., Lawrence, M. G., Montanaro, V., Müller, J.-F., Pitari, G., Prather, M. J., Pyle, J. A., Rast, S., Rodriguez, J. M., Sanderson, M. G., Savage, N. H., Shindell, D. T., Strahan, S. E., Sudo, K. and Szopa, S.: Multimodel ensemble simulations of present-day and near-future tropospheric ozone, J. Geophys.

Res., 111(D8), D08301, doi:10.1029/2005JD006338, 2006.
Stohl, A., Forster, C., Eckhardt, S., Spichtinger, N., Huntrieser, H., Heland, J., Schlager, H., Wilhelm, S., Arnold, F. and Cooper, O.: A backward modeling study of intercontinental pollution transport using aircraft measurements, J. Geophys. Res., 108(D12), 4370, doi:10.1029/2002JD002862, 2003a.
Stohl, A., Wernli, H., James, P., Bourqui, M., Forster, C., Liniger, M. A., Seibert, P. and Sprenger, M.: A New Perspective of Stratosphere–Troposphere Exchange, Bull. Am. Meteorol. Soc., 84(11), 1565–1573, doi:10.1175/BAMS-84-11-1565, 2003b.
Stohl, A., Forster, C., Frank, A., Seibert, P. and Wotawa, G.: Technical note: The Lagrangian particle dispersion model FLEXPART version 6.2, Atmos. Chem. Phys., 5(9), 2461–2474, doi:10.5194/acp-5-2461-2005, 2005.
Struzewska, J. and Kaminski, J. W.: Formation and transport of photooxidants over Europe during the July 2006 heat wave – observations and GEM-AQ model simulations, Atmos. Chem. Phys., 8(3), 721–736, doi:10.5194/acp-8-721-2008, 2008.
Tang, Q., Prather, M. J. and Hsu, J.: Stratosphere-troposphere exchange ozone flux related to deep convection, Geophys. Res. Lett., 38(3), n/a–n/a, doi:10.1029/2010GL046039, 2011.
Thouret, V., Marenco, A., Logan, J. A., Nédélec, P. and Grouhel, C.: Comparisons of ozone measurements from the MOZAIC airborne program and the ozone sounding network at eight locations, J. Geophys. Res., 103(D19), 25695, doi:10.1029/98JD02243, 1998.
Thouret, V., Cammas, J.-P., Sauvage, B., Athier, G., Zbinden, R., Nédélec, P., Simon, P. and Karcher, F.: Tropopause referenced ozone climatology and inter-annual variability (1994–2003) from the MOZAIC programme, Atmos. Chem. Phys., 6(4), 1033–1051, doi:10.5194/acp-6-1033-2006, 2006.
Tiao, G. C., Reinsel, G. C., Pedrick, J. H., Allenby, G. M., Mateer, C. L., Miller, A. J. and DeLuisi, J. J.: A statistical trend analysis of ozonesonde data, J. Geophys. Res., 91(D12), 13121, doi:10.1029/JD091iD12p13121, 1986.
Tressol, M., Ordonez, C., Zbinden, R., Brioude, J., Thouret, V., Mari, C., Nedelec, P., Cammas, J.-P., Smit, H., Patz, H.-W. and Volz-Thomas, A.: Air pollution during the 2003 European heat wave as seen by MOZAIC airliners, Atmos. Chem. Phys., 8(8), 2133–2150, doi:10.5194/acp-8-2133-2008, 2008.
Weatherhead, E. C., Stevermer, A. J. and Schwartz, B. E.: Detecting environmental changes and trends, Phys. Chem. Earth, Parts A/B/C, 27(6-8), 399–403, doi:10.1016/S1474-7065(02)00019-0, 2002.
Wilson, R. C., Fleming, Z. L., Monks, P. S., Clain, G., Henne, S., Konovalov, I. B., Szopa, S. and Menut, L.: Have primary emission reduction measures reduced ozone across Europe? An analysis of European rural background ozone trends 1996–2005, Atmos. Chem. Phys., 12(1), 437–454,

doi:10.5194/acp-12-437-2012, 2012.
Worden, H. M., Deeter, M. N., Frankenberg, C., George, M., Nichitiu, F., Worden, J., Aben, I., Bowman, K. W., Clerbaux, C., Coheur, P. F., de Laat, A. T. J., Detweiler, R., Drummond, J. R., Edwards, D. P., Gille, J. C., Hurtmans, D., Luo, M., Martínez-Alonso, S., Massie, S., Pfister, G. and Warner, J. X.: Decadal record of satellite carbon monoxide observations, Atmos. Chem. Phys., 13(2), 837–850, doi:10.5194/acp-13-837-2013, 2013.
Wu, S., Mickley, L. J., Jacob, D. J., Logan, J. A., Yantosca, R. M. and Rind, D.: Why are there large differences between models in global budgets of tropospheric ozone?, J. Geophys. Res., 112(D5), D05302, doi:10.1029/2006JD007801, 2007.
Zbinden, R. M., Cammas, J.-P., Thouret, V., Nédélec, P., Karcher, F. and Simon, P.: Mid-latitude tropospheric ozone columns from the MOZAIC program: climatology and interannual variability, Atmos. Chem. Phys., 6(4), 1053–1073, doi:10.5194/acp-6-1053-2006, 2006.
Zbinden, R. M., Thouret, V., Ricaud, P., Carminati, F., Cammas, J.-P. and Nédélec, P.: Climatology of pure tropospheric profiles and column contents of ozone and carbon monoxide using MOZAIC in the mid-northern latitudes (24° N to 50° N) from 1994 to 2009, Atmos. Chem. Phys., 13(24), 12363–12388, doi:10.5194/acp-13-12363-2013, 2013.
Zellweger, C., Hüglin, C., Klausen, J., Steinbacher, M., Vollmer, M. and Buchmann, B.: Inter-comparison of four different carbon monoxide measurement techniques and evaluation of the long-term carbon monoxide time series of Jungfraujoch, Atmos. Chem. Phys., 9(11), 3491–3503, doi:10.5194/acp-9-3491-2009, 2009.